1-1-2020

Adaptive in vivo device for theranostics of inflammation: Real-time monitoring of interferon-γ and aspirin

Chaomin Cao
Huazhong Normal University

Ronghua Jin
Xi'an Jiaotong University

Hui Wei
Huazhong Normal University

Zhongning Liu
Peking University Hospital of Stomatology

Shengnan Ni
Huazhong Normal University

See next page for additional authors

Acta Biomaterialia 101 (2020) 372–383

Contents lists available at ScienceDirect

Acta Biomaterialia

journal homepage: www.elsevier.com/locate/actbio

Adaptive *in vivo* device for theranostics of inflammation: Real-time monitoring of interferon-γ and aspirin

Chaomin Cao[a,1], Ronghua Jin[b,1], Hui Wei[a], Zhongning Liu[d], Shengnan Ni[a], Guo-Jun Liu[e], Howard A. Young[f], Xin Chen[b,*], Guozhen Liu[a,c,*]

[a] *International Joint Research Center for Intelligent Biosensor Technology and Health, Central China Normal University, Wuhan 430079, PR China*
[b] *School of Chemical Engineering and Technology, Shanxi Key Laboratory of Energy Chemical Process Intensification, Institute of Polymer Science in Chemical Engineering, Xi'an Jiao Tong University, Xi'an 710049, PR China*
[c] *Graduate School of Biomedical Engineering, ARC Centre of Excellent for Nanoscale Bipphotonics, Faculty of Engineering, The University of New South Wales, Sydney NSW 2052, Australia*
[d] *Department of Prosthodontics, National Clinical Research Center for Oral Diseases, National Engineering Laboratory for Digital and Material, Technology of Stomatology, Beijing Key Laboratory of Digital Stomatology, Peking University School and Hospital of Stomatology, Beijing 100081, PR China*
[e] *Australian Nuclear Science and Technology Organization, New Illuwarra Road, Lucas Heights, NSW 2234, Australia*
[f] *Cancer and Inflammation Program, Center for Cancer Research, National Cancer Institute at Frederick, Frederick, MD 21702, United States*

ARTICLE INFO

Article history:
Received 26 April 2019
Revised 20 September 2019
Accepted 11 October 2019
Available online 15 October 2019

Keywords:
Cytokines
Adaptive *in vivo* device
Structure-switching aptamers
Theranostics
Inflammation
Aspirin
Interferon-γ (IFN-γ)

ABSTRACT

Cytokines mediate and control immune and inflammatory responses. Complex interactions exist among cytokines, inflammation, and the innate and adaptive immune responses in maintaining homeostasis, health, and well-being. On-demand, local delivery of anti-inflammatory drugs to target tissues provides an approach for more effective drug dosing while reducing the adverse effects of systemic drug delivery. This work demonstrates a proof-of-concept theranostic approach for inflammation based on analyte-kissing induced signaling, whereby a drug (in this report, aspirin) can be released upon the detection of a target level of a proinflammatory cytokine (*i.e.*, interferon-γ (IFN-γ)) in real time. The structure-switching aptamer-based biosensor described here is capable of quantitatively and dynamically detecting IFN-γ both *in vitro* and *in vivo* with a sensitivity of 10 pg mL^{-1}. Moreover, the released aspirin triggered by the immunoregulatory cytokine IFN-γ is able to inhibit inflammation in a rat model, and the release of aspirin can be quantitatively controlled. The data reported here provide a new and promising strategy for the *in vivo* detection of proinflammatory cytokines and the subsequent therapeutic delivery of anti-inflammatory molecules. This universal theranostic platform is expected to have great potential for patient-specific personalized medicine.

Statement of Significance

We developed an adaptive *in vivo* sensing device whereby a drug, aspirin, can be released upon the detection of a proinflammatory cytokine, interferon-γ (IFN-γ), in real time with a sensitivity of 10 pg mL^{-1}. Moreover, the aspirin triggered by IFN-γ depressed inflammation in the rat model and was delivered indirectly through blood and cerebrospinal fluid or directly to the inflammation tissue or organ without adverse gastrointestinal effects observed in the liver and kidney. We envision that, for the first time, patients with chronic inflammatory disease can receive the right intervention and treatment at the right time. Additionally, this technology may empower patients to monitor their personalized health and disease management program, allowing real-time diagnostics, disease monitoring, and precise and effective treatments.

1. Introduction

Inflammation is a self-protection defense mechanism that is critical to combat harmful stimuli (*e.g.*, pathogens) and initiate the healing process. However, under many conditions, the inflammatory response becomes chronic and leads to significant

* Corresponding author.
E-mail addresses: chenx2015@xjtu.edu.cn (X. Chen), guozhen.liu@unsw.edu.au (G. Liu).
[1] Chaomin Cao and Ronghua Jin contributed equally to this work.

https://doi.org/10.1016/j.actbio.2019.10.021
1742-7061/

tissue/organ damage. [1] Recently, increasing evidence demonstrates that an abnormal inflammatory response is closely associated with many cancers [2] and numerous autoimmune diseases [3] including rheumatoid arthritis, atherosclerosis, inflammatory bowel disease, systemic lupus erythematosus, type 2 diabetes, and Alzheimer's disease. Inflammation is caused by a number of physiological reactions triggered by the immune system in response to a physical injury or an infection. However, the precise source of the inflammatory stimulus is often unknown and, even if known, may be difficult to remove or inhibit. Thus, interest has been shown toward therapeutically targeting the inflammatory response to inhibit and limit disease progression. Ongoing disease management in the context of chronic inflammation is increasing, with major unmet needs in the era of precision diagnostics and treatment. [4] Although there has been success with anti-inflammatory therapy in chronic diseases such as rheumatoid arthritis, there are considerable limitations because of the toxicity associated with treatment and variation in patient response. In particular, as the inflammatory response is critical for host homeostasis, the challenges of redundancy, compensation by the host, and the necessity for basal immune function often narrow the risk-to-benefit ratio of anti-inflammatory drugs. Thus, it is essential for patients with chronic inflammatory disease to receive treatments that target the abnormal immune response in a timely and precise manner.

Precision medicine is a medical model that aims for the customization of healthcare with medical decisions, practices, and products tailored to the individual patient. On the basis of the knowledge of disease mechanisms, precision medicine generally combines diagnosis and treatment to achieve optimal disease management [5]. The paradigm of intelligent personalized medicine holds the promise to revolutionize healthcare by delivering "the right drug, at the right dose, and at the right time" [6]. As stated above, precision medicine is particularly important in addressing individual inflammation [7] and inflammation-based diseases [8]. To meet the needs of precision medicine with an approach that can be applied to many individuals without the need for specialized and costly individualized therapies, we report here the development of a technology that meets this targeted goal.

In this report, we have utilized aptamer technology to monitor and measure the host inflammatory response. Aptamers are oligonucleotides or peptides that can bind to their targets with high affinity and specificity [9]. Aptamers, as a potent and specific alternative to antibodies, not only have all of the advantages of specific interactions with their target molecules but also have unique merits including thermal stability, low production cost, lack of immunogenicity, ease of chemical synthesis and modification, rapid tissue penetration, and unlimited applications in diagnostics and therapeutics [10]. Aptamer beacons can reversibly load and release a molecular cargo upon binding to a specific target analyte [11]. This feature can be deployed for real-time sensing, [12–14] computing, actuating, or drug delivery [15–17], thus moving aptamer-based precision medicine closer to reality. For example, Ricci and coworkers demonstrated the construction of a modular DNA-based nanomachine that can reversibly load and release the nucleic acid upon binding to a specific antibody. [18] The antibody-powered DNA nanomachines have demonstrated great potential in applications including controlled drug release, point-of-care diagnostics, and personalized medicine. [19]

Cytokines, which act as mediators and modulators in the differentiation, sensitization, and activation of various immune cells, are bioactive soluble proteins produced by the immune and nonimmune cells that are directly required for normal host immune function as well as disease initiation and progression [20,21] The elevated concentration of cytokines in the host serum or at specific locations (e.g., a solid tumor) normally indicates the activation of inflammation or other steps in disease progression [22]. Thus, for patients with chronic inflammatory disease or cancer to receive treatment at the right time, it will be essential to monitor cell functions and cell-to-cell communication, as measured by cytokine expression, and then initiate precision drug delivery according to the *in vivo* cytokine concentration. However, there are many challenges in meeting this objective, including the fact that cytokine-related immune reactions are often extremely dynamic and may be transient and/or localized in nature. [22] In addition, cytokines are either not detectable or only expressed at picomolar concentrations in body fluid or tissues of healthy individuals. We have successfully achieved the sensitivity in pg mL^{-1} range of cytokine measurement by introducing nanomaterials to the sensing interfaces. [23–25] To realize real-time detection of cytokines, we have developed different sensing platforms based on aptamers for the detection of cytokines. [26,27] Taking advantage of the structure-switching property of aptamers, we recently reported a structure-switching aptamer-based recyclable *in vivo* sensing device for the continuous detection of the cytokine IFN-γ in mice at a sensitivity of 1 pg mL^{-1}. [28] In this system, redox probes were loaded in the hairpin part of the aptamer, which were released upon the detection of IFN-γ. It was observed that the released redox probes could be reloaded to aptamers to realize the regeneration of the sensing interfaces. Inspired by this system, we are interested in developing a smart stimuli-responsive system that can enable continuous cytokine monitoring with a high sensitivity while drug delivery is triggered when *in vivo* cytokine levels reach a pathological or "alarmed" level.

Nonsteroidal anti-inflammatory drugs such as aspirin are among the earliest agents used in western medicine. Pharmacological effects of aspirin are thought to occur through covalent modification of cyclooxygenase (COX) [29]. In this report, we developed an adaptive *in vivo* sensing devices (Fig. 1) based on a glassy carbon (GC) rod, which provides an approach whereby a drug, aspirin, can be released upon the detection of a target level of the proinflammatory cytokine interferon-γ (IFN-γ) in real time. The sensor described here is capable of quantitatively and dynamically detecting IFN-γ both *in vitro* and *in vivo* at a sensitivity of 10 pg mL^{-1}. Moreover, the released aspirin triggered by IFN-γ depresses inflammation in a rat model. We demonstrate here that aspirin loaded in aptamers and delivered indirectly through blood and cerebrospinal fluid or directly to a tissue or organs can avoid adverse gastrointestinal effects and other adverse effects observed in the liver and kidney. With our approach, we aim, for the first time, that patients with chronic inflammatory disease can receive the right intervention and treatment at the right time. Additionally, this technology may empower patients to precisely monitor their personalized health and disease management through real-time diagnostics and disease/treatment monitoring.

2. Experimental section

2.1. Chemical and materials

Aspirin, streptavidin, Tris(hydroxymethyl)aminomethane (Tris), hydrochloric acid, potassium chloride, magnesium chloride, sodium nitrite, potassium ferricyanide, 1-ethyl-3-(3-dimethylaminopropyl)carbodiimidehydrochloride (EDC), 4-carboxyphenyl aryldiazonium salt, N-hydroxysuccinimide (NHS), 2-(N-morpholino)ethanesulfonic acid (MES), and lipopolysaccharide (LPS) were purchased from Sigma-Aldrich. Phosphate buffer solution contained 0.05 M KCl and 0.05 M K_2HPO_4/KH_2PO_4 adjusted to pH 7.4 with NaOH or HCl solution. Aqueous solutions were prepared using Milli-Q water. Recombinant human IFN-γ was purchased from R&D Systems (Minneapolis, MN, USA). All DNA was produced by Shanghai Sangon Biotech Co. Ltd. (Shanghai, China). The sequence of the hairpin aptamer probe (red color is

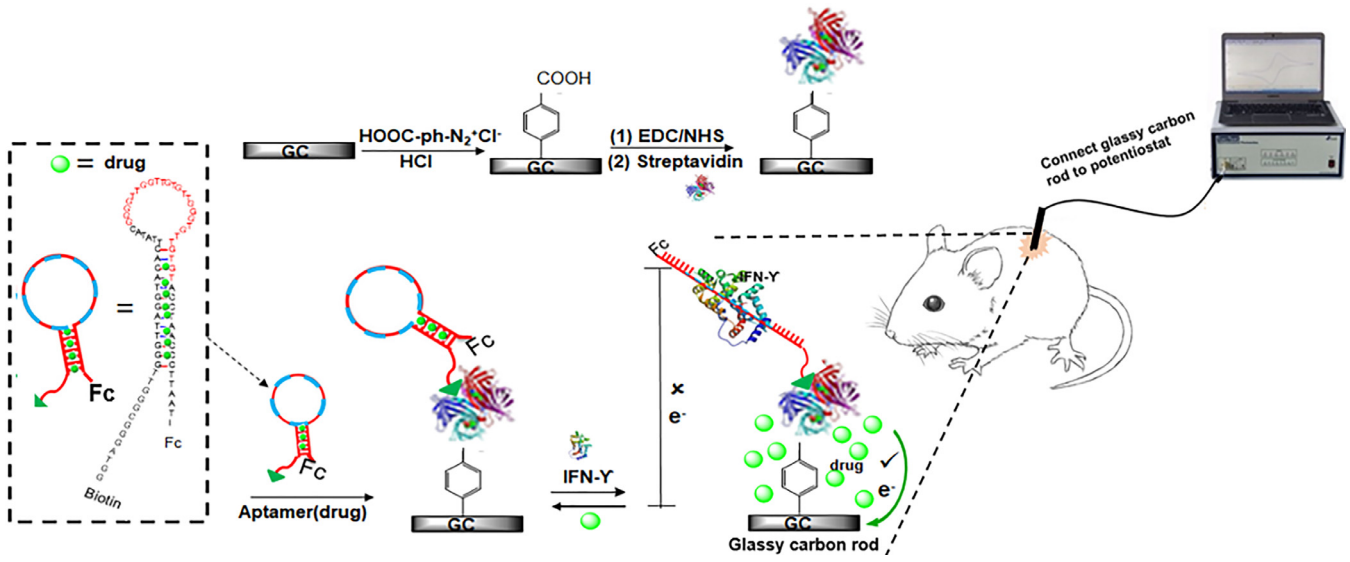

Fig. 1. Schematic of the fabricated adaptive *in vivo* device for monitoring IFN-γ and IFN-γ-triggered drug delivery.

the sequence that has affinity to both human and murine IFN-γ) was 5′-Fc-C_6-GGG GTT GGT TGT GTT GGG TGT GTC CAA CCC C-C_3-biotin-3′. Tris-HCl buffer contained 100 mM Tris-HCl, 100 mM NaCl, 1 mM $MgCl_2$, and 5 mM KCl, pH at 7.4.

2.2. Apparatus

All electrochemical experiments were conducted with CHI660E (CH Instruments, Inc., Shanghai). GC electrodes were 3 mm disks embedded in epoxy resin (Gaoss Union, China). All experiments used a Pt secondary electrode and an SCE (saturated calomel electrode) reference electrode. X-ray photoelectron spectra (XPS) were recorded from GC plates on a VG MultiLab 2000 spectrometer with a monochromatic Al Kα source, hemispherical analyzer, and multichannel detector. The spectra were analyzed using XPSPEAK41 software. UV–Vis absorption data were recorded on a Shimadzu UV–Vis spectrophotometer model 2450.

2.3. Preparation of aptamer(aspirin) probes

To prepare the aptamer(aspirin) probes, 100 µL of 20 µM aspirin-containing water solution was mixed with 100 µL of 5 µM IFN-γ aptamer probe solution, and the mixture solution was incubated in Tris-HCl buffer solution (pH = 7.4) at room temperature for 24 h. After reaction, the sample was filtered using a centrifugal filter (Millipore, Amicon Ultra-0.5 mL 30 K) to wash and purify the aptamer (aspirin). The achieved aptamer(aspirin) probes were stored at 4 °C before use.

2.4. Preparation of the sensing interface for detection of IFN-γ

The GC electrodes were cleaned by being hand-polished on microcloth pads in 1.0, 0.3, and 0.05 µm alumina slurries in succession (made from dry alumina and water), and then they were thoroughly rinsed with water and sonicated in water for 1 min. Before modification with aryldiazonium salts, the GC electrode was dried under a stream of nitrogen followed by exposure to 0.5 M HCl solution containing 1 mM corresponding diazonium salts, which was degassed for 15 min with nitrogen flow in an ice bath. The electrochemical reductive modification of the GC electrodes with 4-carboxyphenyl (HOOC-ph-GC) was achieved by scanning in the potential range from 0.6 V to −1.0 V for 2 cycles with a scan rate of 100 mV s^{-1}. After washing with water and finally drying under a stream of nitrogen, the carboxylic group-terminated GC surfaces (GC-ph-COOH) were immersed in 10 mM EDC and 40 mM NHS prepared in 100 mM MES buffer solution for 1 h to activate the carboxylic acid group on the electrode surface. After rinsing with deionized water and Tris-HCl buffer solution, the activated electrodes were dried under N_2, followed by incubation in 200 µg mL^{-1} streptavidin (STR) in pH=7.4 Tris-HCl buffer solution at room temperature for 4 h to obtain GC-ph-STR surfaces. Finally, GC-ph-STR surfaces was immersed into 5 µM aptamer(aspirin) solution for 1 h to generate GC-ph-STR-aptamer(aspirin) surfaces for the detection of IFN-γ.

2.5. Electrochemistry measurement of IFN-γ using the aptamer(aspirin)-modified sensing interface

The prepared GC-ph-STR-aptamer(aspirin) surfaces were incubated with 10 µL Tris-HCl buffer containing IFN-γ at various concentrations for 30 min at room temperature. Then the squarewave voltammetry (SWV) of aptamer(aspirin)-modified GC electrodes after exposure to IFN-γ was collected using a CHI660E workstation by scanning the potential between −0.2 V and 1.2 V with a step potential of 4 mV, a frequency of 10 Hz, and an amplitude of 40 mV. Real-time measurement was carried out by chronoamperometry in a series of different concentrations of IFN-γ by fixing the potential at 0.2 V for 5000 s for Fc and 0.9 V for 5000 s for aspirin.

2.6. Cell culture

Informed consent in this study was obtained under approved Animal Research Ethics Committee protocols with the ethics number 2017065. Peripheral blood mononuclear cells (PBMCs) were purchased from Procell (Wuhan, China). The cells were cultured in a T25 cm^2 flask in RPMI-1640 medium supplemented with 10% heat-inactivated human serum AB, 10 U mL^{-1} of penicillin, 1000 U mL^{-1} IL-2, 1100 µg mL^{-1} of streptomycin,10 µg mL^{-1} gentamicin, 2 mM gentamine, and 25 mM HEPES. The cells, at a concentration of 1×10^6/mL, were incubated in a 6-well plate at 37 °C and 5% CO_2. To harvest, the cells at 80–90% confluence were washed twice with Dulbecco's phosphate-buffered saline, followed by trypsinization using 2 mL of trypsin to detach the cells from the flask. The trypsin was neutralized by adding 4 mL of fresh supplemented medium, and the harvested cells were resuspended in complete RPMI-1640 medium, transferred into a centrifuge

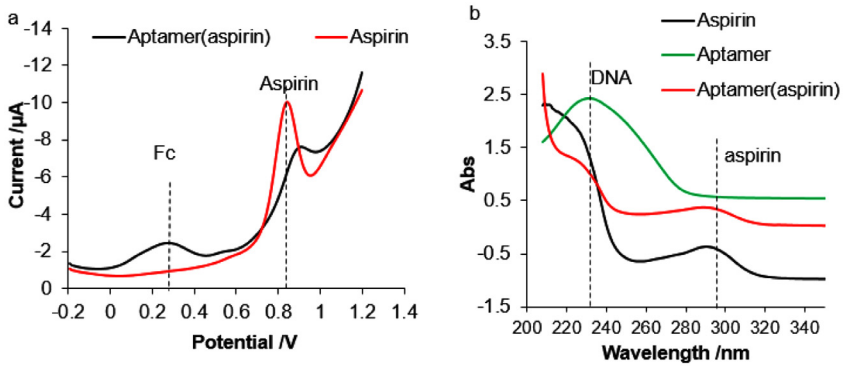

Fig. 2. (a) Electrochemistry of aptamer(aspirin) probes and aspirin in pH = 7.4 Tris–HCl buffer solution. (b) UV–Vis spectra of aptamer (5 μM), aspirin (50 μM), and aptamer(aspirin) (5 μM) in pH = 7.4 Tris–HCl buffer solution.

tube, and centrifuged at 1500 rcf for 10 min. The supernatant was discarded, and the cells were resuspended in fresh medium. For the preparation of IFN-γ samples, the cells at a density of 1×10^6/mL were suspended in 1 mL of warm complete medium containing 0.1 μg mL^{-1} LPS to induce IFN-γ expression at 0 h, 2 h, 4 h, 6 h, 8 h, and 20 h. The supernatants from cells were collected in triplicate. The Nunc MaxiSorp 96-well plate and the Galaxy plate reader were used for subsequent ELISA.

2.7. Animal model of endotoxemia

Adult wild-type Sprague Dawley male rats were purchased from Vital River Corporation (Beijing, China). The rats were randomly divided into two groups (number of animals/group) as (1) the control group (no electrode implant) and (2) the electrode implant group for corresponding time points at 0 h, 1 h, 6 h, 12 h, and 24 h after induction of endotoxemia. Surgery was performed under anesthesia by inhalation of 4% isofluorane, and the animals were maintained in 2% isofluorane. To induce endotoxemia, LPS (5 mg/kg) was injected intraperitoneally. After injection, the aspirin-loaded electrodes were implanted into the subcutaneous pockets on the back of the animals, and the skin was closed with sutures. The animals were euthanized with CO_2 at 0 h, 1 h, 6 h, 12 h, and 24 h, and the blood and electrodes were harvested for analysis. As the lung is the moderately affected tissue in endotoxemia, the lungs were collected for histological analysis at 24 h.

2.8. ELISA assays

To evaluate the effects of aspirin-loaded electrodes, the blood specimens of the two groups of rats and the interstitial fluid of the lung were collected and processed immediately for further cytokine measurement. The levels of inflammatory cytokines (IL-6 and IFN-γ) in the serum and fluid were measured using the enzyme-linked immunosorbent assay (ELISA) kit (Boster Biological Technology, China) according to the manufacturer's instructions.

2.9. Histology and immunohistochemistry assay

The lungs from experimental groups of rats were collected, fixed in 10% formalin overnight, embedded in paraffin, and sectioned at a thickness of 5 μm. The sections were deparaffinized, rehydrated, and stained with hematoxylin and eosin (H&E). Moreover, the sections were also stained with a neutrophil marker (Ly-6 G antibody, Thermo Fisher Scientific, USA) for immunohistochemistry measurement. The procedure was carried out according to the protocol of the atreptavidin-peroxidase immunohistochemical kit with antimouse Ly-6 G/Gr-1 antibodies (1:200, Santa Cruz Biotechnology), followed by antimouse IgG-horseradish peroxidase-conjugated secondary antibody (1:200, Jackson), and the 3,3′-diaminobenzidine (DAB) coloration kit (Zhongshan Bioengineering Co. Ltd, Beijing, China). The immunostaining results were observed after samples were treated with a hematoxylin counterstain. For histopathological analyses, four inflammatory parameters were scored independently from 0 to 4 for each section as previously described [30]: alveolar congestion; (b) hemorrhage; (c) neutrophilic infiltration, and (d) thickness of the alveolar wall and hyaline membrane formation. Each category was graded on a 0- to 4-point scale: 0 = no injury; 1 = injury up to 25% of the field; 2 = injury up to 50% of the field; 3 = injury up to 75% of the field; and 4 = diffuse. [31] Injury slides were randomized, read blindly, and scored for each. The inflammatory cell number and the positive area of IHC staining were evaluated with Image-Pro-Plus software.

2.10. Statistical methods

All experiments were performed in at least triplicate, and the results were presented as the mean and standard deviation of the three replicates. Statistical analyses were performed with both Excel and Origin. We considered $p < 0.01$ as statistical significance.

3. Results and discussion

3.1. Characterization of aptamer (aspirin) probes

Initially, the SWVs of GC electrodes in pH=7.4 Tris-HCl buffer solution after applying 10 μL of 20 μM aspirin, 5 μM aptamer, and 5 μM aptamer(aspirin) probe were determined. As shown in Fig. 2, a pair of redox peaks was observed for GC electrodes after applying the aspirin solution at 0.9 V. However, two pairs of peak current were observed after applying the aptamer(aspirin) probe on the GC electrode at 0.2 V and 0.9 V, representing ferrocene and aspirin, respectively, suggesting that aspirin has been embedded into the stem part of the aptamer probe as shown in the schematic design in Fig. 1. This result was confirmed by UV–Vis absorption spectroscopy (Fig. 2b), as one absorption peak, centered at 260 nm, was observed in the UV–Vis absorption spectra of aptamer and aptamer (aspirin). Another absorption peak, centered at 295 nm, was observed in the UV–Vis absorption spectra of both aspirin and aptamer (aspirin) [32]. This result suggested that aspirin was successfully intercalated into the double-stranded 5′-GC-3′ sequences of the aptamer by the force of π–π stacking to confirm the aptamer (aspirin) probes [33]. Under optimized conditions, we quantified the number of aspirin molecules loaded on the aptamer

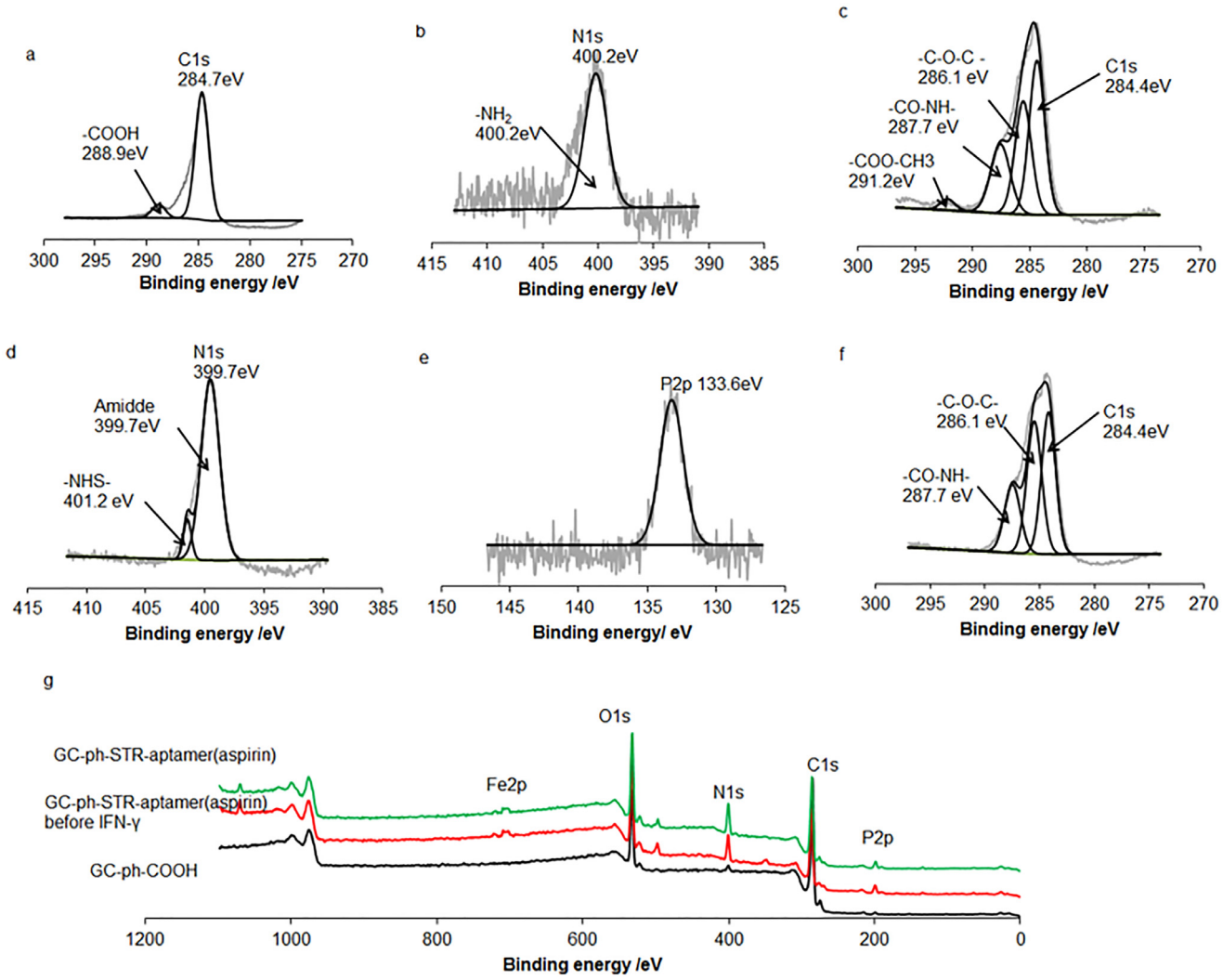

Fig. 3. (a) C1s spectra for GC-ph-COOH. (b) N1s spectra for GC-ph-COOH. (c) C1s spectra for GC-ph-STR-aptamer(aspirin). (d) N1s spectra for GC-ph-STR-aptamer(aspirin). (e) P2p spectra for GC-ph-STR-aptamer(aspirin). (f) GC-ph-STR-aptamer(aspirin) after exposure to 500 pg mL^{-1} IFN-γ for 30 min followed by washing. (g) XPS survey spectra for stepwise modification of the sensing interfaces.

complex according to the modified protocol [34]. Supplementary Figure S1 shows the SWV curves that were obtained by reacting 100 µL of 5 µM aptamer solution with different concentrations of 100 µL aspirin solution for 24 h. The oxidation peak current of aspirin increased with the increase in the concentration of aspirin from 5 to 100 µM, and it reached a plateau when a concentration of more than 20 µM was added. Thus, the optimized concentration of the aspirin solution was 20 µM (Supplementary Figure S1 a). On the basis of the calibration curve between aspirin concentration and absorbance (Supplementary Figure S1 b), the maximal absorbance of the aspirin was observed when the ratio of aspirin and aptamer reached 3:1, suggesting three aspirin molecules could intercalate into one aptamer. To provide more information about the loading capacity of aspirin on each electrode, the optimized electrode was heated to 95 °C to release all the encapsulated aspirin as a result of DNA denaturation. The released aspirin was measured by UV–Vis absorption spectroscopy, indicating the amount of aspirin on each electrode was approximately 3.1 µmol.

3.2. XPS characterization of the stepwise fabricated sensing interface

XPS measurements were carried out to further characterize GC surfaces after stepwise modification with different species. C1s has two peaks at around 284.7 eV and 288.9 eV. The peak at 288.9 eV is assigned to the carbon of the carboxyl groups on the surface of GC-ph-COOH (Fig. 3a) [35]. However, N1s has two peaks at about 400.2 eV, which are assigned to unreacted carboxyphenyl (Fig. 3b). For the GC-ph-STR-aptamer(aspirin) surface, C1s has four peaks at around 284.4 eV, 286.1 eV, 287.7 eV, and 291.2 eV (Fig. 3c). The peak at 286.1 eV is assigned to the –C–O–C- species in streptavidin [36]. The peak at 287.7 eV is assigned to the peptide bond formed by the interaction between -COOH from 4-carboxyphenyl on electrodes and amine from streptavidin [26]. The peak at 291.2 eV is assigned to the -COO–CH_3- species in aspirin [33]. In addition, the peak at 133.6 eV was assigned to phosphorus in the aptamer DNA (Fig. 3e) [37]. The results suggest that aptamer(aspirin) was successfully attached onto the GC-ph-COOH surface. However, two peaks at 399.7 eV and 401.2 eV were observed in the N1 species on the GC-ph-STR-aptamer(aspirin) surfaces, and these were assigned to unreacted EDC and NHS, respectively (Fig. 3d). However, the peak of C1s at 291.2 eV disappeared after exposure of the aptamer(aspirin)-modified GC surfaces to 500 pg mL^{-1} IFN-γ, suggesting that the GC-ph-STR-aptamer(aspirin) surfaces could release aspirin in the presence of IFN-γ (Fig. 3f). Fig. 3g illustrates XPS survey spectra confirming the successful stepwise modification of the sensing interfaces.

3.3. Electrochemistry characterization of the stepwise fabricated sensing interface

The stepwise fabrication of the GC-ph-STR-aptamer(aspirin) sensing surfaces was also characterized by electrochemistry. The first sweep of the electrochemical modification of GC with the 4-carboxyphenyl groups (Supplementary Figure S1 c) produced an irreversible reduction wave at −0.4 V corresponding to the reduction of the carboxyl acid group to a radical anion. On the second scan, the first wave at −0.4 V vanished, suggesting inhibition of the electron transfer by the 4-carboxyphenyl group grafted on the GC surfaces. After the modification of 4-carboxyphenyl layers, the redox peaks of $Fe(CN)_6^{3-}$ observed with bare GC electrodes were completely suppressed (Supplementary Figure S1 d), giving strong evidence that a monolayer of 4-carboxyphenyl, which blocked the access of redox molecules to the GC electrode, had formed on the GC surfaces. The SWV curves of bare GC, HOOC-ph-GC, STR-GC, and aptamer(aspirin)-GC in PBS buffer are displayed in Supplementary Figure S1 e. A redox peak was observed at 0.8 V, which is the characteristic peak of STR, suggesting that STR was successfully modified onto the electrode surface [38]. After modification of the aptamer(aspirin) onto the GC electrode to form aptamer (GC) through the interaction between biotin and streptavidin, a symbolic peak from Fc was observed in SWV (Supplementary Figure S1 f).

3.4. In vitro *real-time monitoring of IFN-γ and IFN-γ-triggered aspirin release using the GC-ph-STR-aptamer (aspirin) interface*

After the successful fabrication of the GC-ph-STR-aptamer(aspirin) sensing interface, the electrochemical response of the GC-ph-STR-aptamer(aspirin) sensing interface to IFN-γ was analyzed (Fig. 4). In the absence of IFN-γ, there was an obvious redox peak observed at 0.2 V, which belongs to a ferrocene-free aptamer (Fig. 4a). According to the redox peak of Fc in Fig. 4a, the surface coverage of the aptamer was calculated to be 5.1 x However, the peak at 0.2 V disappeared, and a pair of redox peaks at approximately 0.9 V, characteristic of aspirin, appeared after exposure to IFN-γ followed by extensive washing. The electrochemical signal switching was due to the binding of IFN-γ to the loop part of the aptamer, leading to the opening of the stem part of aptamer, followed by the subsequent release of aspirin molecules into the environment. This then induced the electric communication between the released aspirin and the underneath GC electrode, resulting in the subsequent Faradic current at 0.9 V. Furthermore, Fc redox molecules labeled on aptamers were dissociated away from the electrode surface because of the configuration change of the aptamer, resulting in decreased electron transfer efficiency between the aptamers and underlying electrodes and, consequentially, switching off of the current. To confirm this hypothesis, SWV, as a more sensitive electrochemical technique, was used to quantitatively monitor the electrochemical response (Fig. 4b).

The real-time sensor described here is based on analyte-kissing-induced structure-switching aptamers and subsequent aspirin-releasing signaling molecules. Thus, any factors that affect the binding of aspirin to the aptamer will contribute to the sensor performance. To investigate environmental influences on the sensor, the effect of pH, salt concentration, and temperature on the stability of the GC-ph-STR-aptamer(aspirin) sensing interface (the release of aspirin) was analyzed (Supplementary Fig. S2). It was observed that under acidic conditions, the DNA was deprived of purines leading to the release of aspirin. Thus, less aspirin was released after reaction with IFN-γ, resulting in a smaller current. However, when the pH reached 8 (Supplementary Fig. S2 a), the aptamer was denatured by the alkaline condition, and that neutralized the charge of acids but caused the hydrolysis of bases upon prolonged treatment. Consequently, pH 7.4 was found to be the optimized condition required to monitor IFN-γ levels. The sensing provided the optimized performance when the salt concentration was 100 mM (Supplementary Figure S2 b). In addition, increasing the temperature from 25 °C to 95 °C also caused the release of aspirin molecules before reaction with IFN-γ. Heating the aptamer(aspirin) solution to 95 °C leads to DNA denaturation by separating a double strand into two single strands, thus subsequently releasing the incorporated aspirin molecules, a process that occurred when the hydrogen bonds between the DNA strands were broken [39]. Consequently, the stem part of the aptamer opens and releases the incorporated aspirin molecules (Supplementary Figure S2 c). However, the GC-ph-STR-aptamer(aspirin) sensing interface performed well at physiological temperature, i.e., 37 °C, which makes it stable under physiological conditions. The reaction time with IFN-γ was also investigated by monitoring the change in current with the reaction time (Supplementary Fig. S2 d). The current increased with the reaction time and reached a plateau when the reaction time was 60 min. The current at 30 min was approximately 90% of that observed at 60 min and thus was selected as the optimized reaction time. Under optimized conditions, the peak current corresponding to IFN-γ decreased with the increase in IFN-γ concentration (Fig. 4c). There was a linear range of 10–500 pg mL^{-1} for the detection of IFN-γ with the lowest detection limit of 10 pg mL^{-1} in Tris buffer. As determined from the midpoint of the IFN-γ calibration curve shown in Fig. 4d, the affinity constant between IFN-γ (molecular weight 16.9 kDa) and the aptamer(aspirin) was calculated to be approximately $5.3 \times 10^{10}\ M^{-1}$. The typical affinity constant K_a for antigen–antibody reactions is in the range of 10^8 to 10^{12} M^{-1} [40], and hence, the data presented here indicate that the aptamer(aspirin) probe has a very high affinity to IFN-γ. Furthermore, the electrochemistry responsible for the released aspirin was recorded (Fig. 4e), and the SWV peak current increased with increasing IFN-γ concentration. The peak current at approximately 0.9 V demonstrated a linear relationship with the concentration of IFN-γ in the range of 0–500 pg mL^{-1}. This observation indicates that aspirin was released, which can be quantitatively measured according to the current change in 0.9 V. This further confirms that our proof-of-concept system for cytokine detection and cytokine-triggered drug delivery was effective.

To investigate the real-time sensing capability of the GC-ph-STR-aptamer(aspirin) interface, a chronoamperometry experiment at a constant potential of 0.2 V (close to the oxidation potential of Fc) was carried out by adding different concentrations of IFN-γ under constant stirring (Fig. 5a). Fig. 5b shows the calibration curve based on the chronoamperometry measurement. The linear range obtained here was 10–500 pg mL^{-1}, which is comparable to that obtained by SWV as shown in Fig. 3d. Upon the addition of IFN-γ, the monitored current of the GC-ph-STR-aptamer(aspirin) sensing interface decreased with the increase of the IFN-γ concentration. A chronoamperometry experiment at a constant potential of 0.9 V (close to the oxidation potential of aspirin) was carried out by adding different concentrations of IFN-γ under constant stirring (Fig. 5c). Upon the addition of IFN-γ, the monitored current of the GC-ph-STR-aptamer(aspirin), in contrast to the current observed by a constant potential of 0.2 V, increased with increasing IFN-γ concentration. This suggests that the presence of IFN-γ induced the configuration change of the aptamer and the subsequent release of aspirin, resulting in increased current at 0.9 V. To confirm the proposed mechanism of the analyte-induced drug delivery, we measured the rate of aspirin release in the presence of IFN-γ. According to Chow's method [41], the drug release rate can be calculated using the equation $K = \ln(C/C_0) / (t\text{-}t_0)$. In the presence of IFN-γ, the rate of aspirin release was calculated to be 0.033 μM min^{-1}, suggesting a quantitatively controlled drug release.

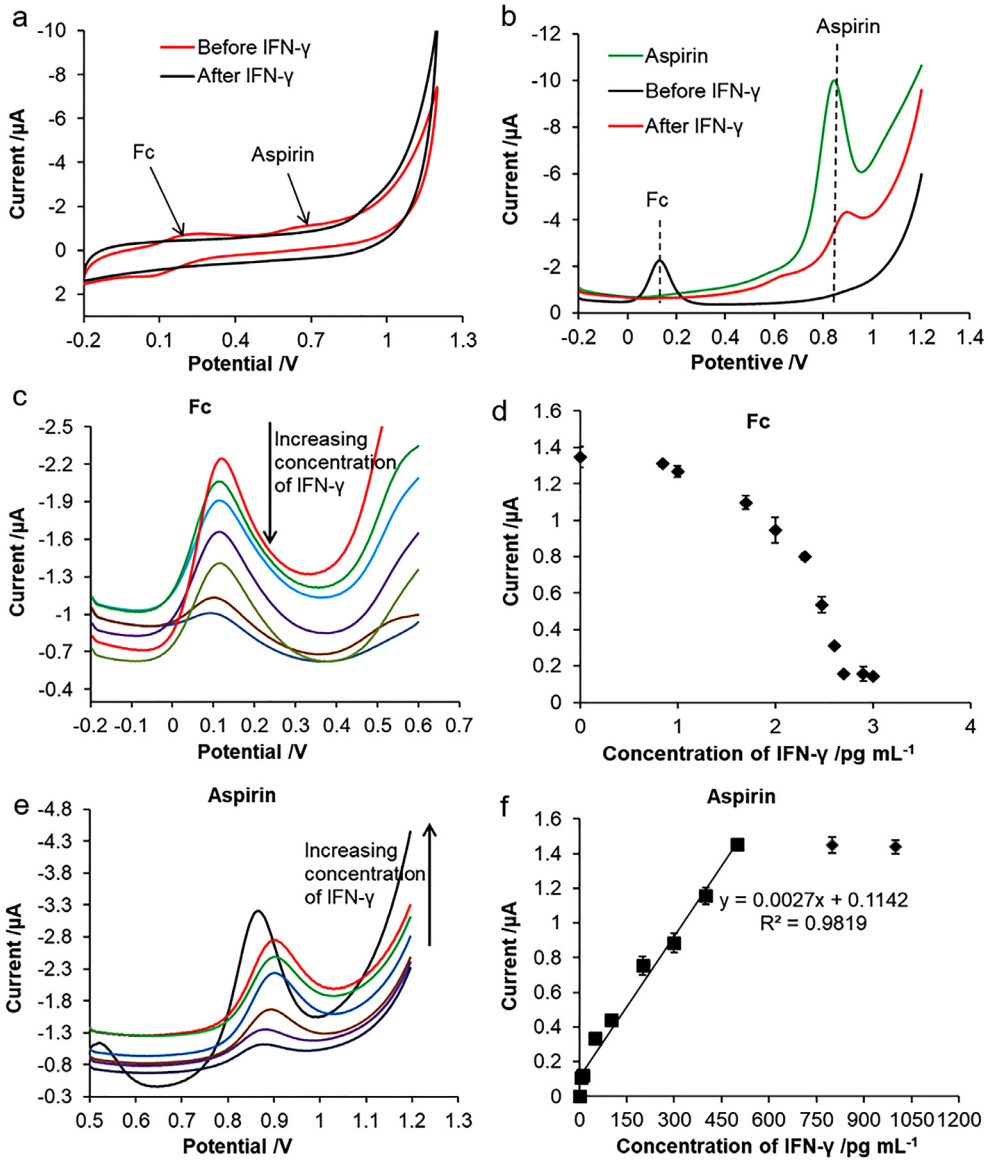

Fig. 4. (a) Cyclic voltammetries and (b) Squarewave voltammetries of the GC-ph-STR-aptamer(aspirin) sensing interface in pH 7.4 Tris buffer before and after exposure to 500 pg mL^{-1} IFN-γ. (c) Spectrum of the Fc peak generated by the SWV of GC-ph-STR-aptamer(aspirin) after exposure to different concentrations of IFN-γ (0, 10, 50, 200, 300, 400, 500, 800, and 1000 pg mL^{-1}). (d) The relationship of the peak current of Fc at (c) with the log concentration of IFN-γ. (e) Spectra of the aspirin peak generated by the SWV of GC-ph-STR-aptamer(aspirin) after exposure to different concentrations of IFN-γ. (f) The relationship of the peak current corresponding to aspirin in (e) with the concentration of IFN-γ.

To investigate the selectivity of the fabricated sensor, seven potentially interfering compounds, namely, bovine serum albumin (BSA, 2 mg mL^{-1}), prostate-specific antigen (PSA, 1 μg mL^{-1}), cancer antigen 125 (CA-125, 1 μg mL^{-1}), IL-6 (1 μg mL^{-1}), TNF-α (1 μg mL^{-1}), IFN-α (1 μg mL^{-1}), and IFN-β (1 μg mL^{-1}), were added to the detection buffer solution in the presence of IFN-γ (500 pg mL^{-1}) (Supplementary Figure S2 e). No significant effect from these seven nonspecific proteins was detected. The retained current percentage for all nonspecific proteins was above 90%, suggesting an insignificant degree of interference by these molecules tested in relation to the control (<10%). The stability of the sensing interface was also analyzed by incubating the GC-ph-STR-aptamer(aspirin) sensing interface in Tris buffer for 1, 2, 3, 5, 10, 15, 20, 25, and 30 days at room temperature, respectively. The electrochemistry was monitored at each time point (Supplementary Figure S2 e). Less than 5% of the signal was lost from Fc after 25 days, indicating that the GC-ph-STR-aptamer(aspirin) sensing interface was stable for at least 25 days.

3.5. Detection of IFN-γ in a cellular microenvironment

The GC-ph-STR-aptamer(aspirin) sensing interface was tested for the detection of IFN-γ secreted by PBMCs (Fig. 6). First, a chronoamperometry experiment at a constant potential of 0.2 V was carried out in a medium containing 1×10^6 cells under stirring, to which IFN-γ, at concentrations of 10–1000 pg mL^{-1}, was added (Fig. 6a). It was observed that the current decreased continuously after adding IFN-γ until it reached a plateau when the concentration of IFN-γ was 500 pg mL^{-1}. The calibration curve for real-time measurement of IFN-γ in the cell culture medium was plotted as shown in Fig. 6b. The supernatant of the 1×10^6 PBMCs was collected for IFN-γ analysis after LPS stimulation for 2, 4, 6, 8, and 12 h. The supernatant samples were subsequently analyzed by ELISA and prepared for the GC-ph-STR-aptamer(aspirin) sensing interface. As shown in Fig. 6b, the concentration of IFN-γ increased with the duration of the 10 ng mL^{-1} LPS treatment, and the maximum level of 500 pg mL^{-1} IFN-γ was obtained after

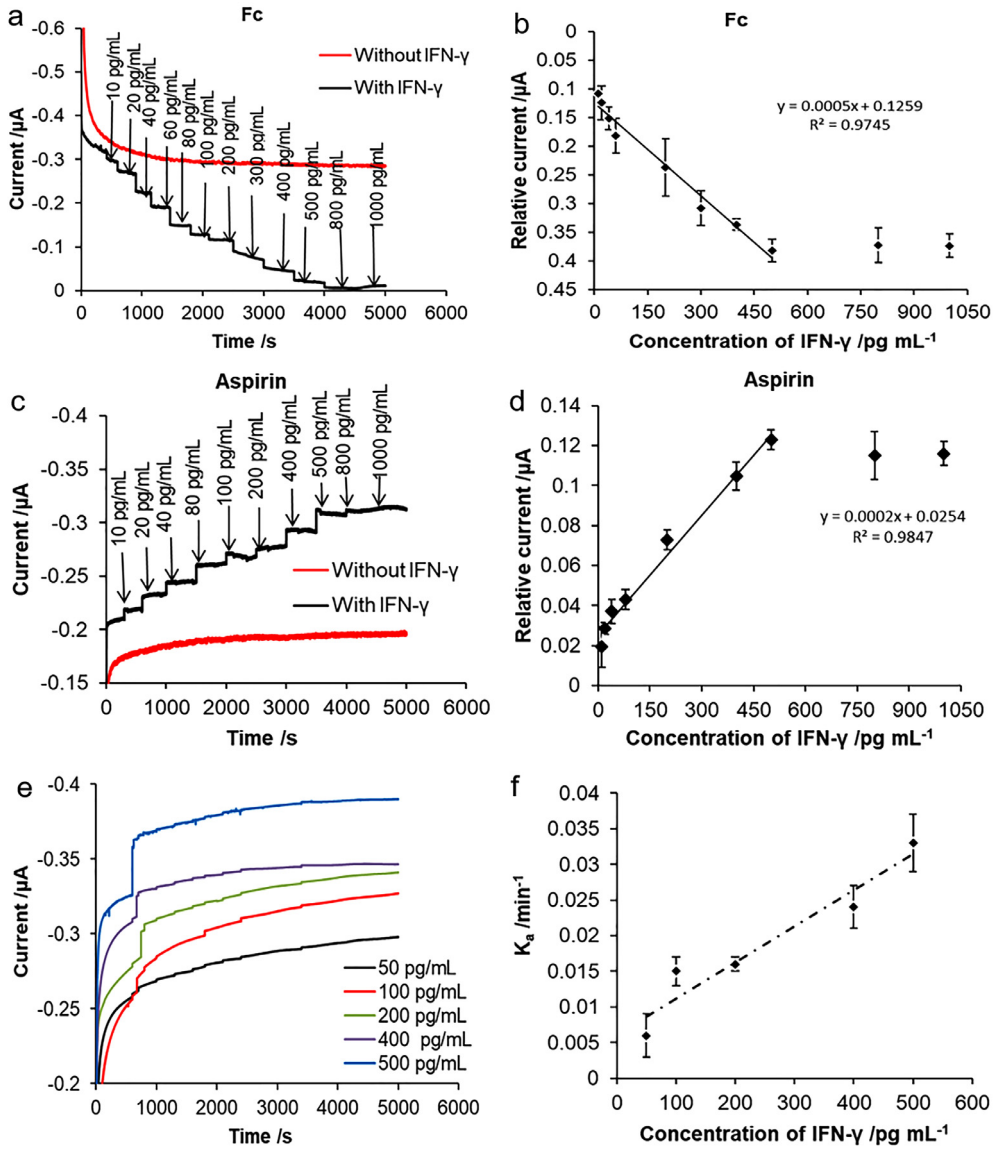

Fig. 5. (a) The current record as a function of time for GC-ph-STR-aptamer(aspirin) in pH = 7.4 Tris–HCl buffer solution at a constant potential of 0.2 V after adding IFN-γ at different concentrations. (b) The calibration curve of the GC-ph-GO-aptamer (Ru) sensing interface obtained by the chronoamperometry in (a) and another two independent measurements. (c) The current record as a function of time for GC-ph-STR-aptamer(aspirin) in pH = 7.4 Tris–HCl buffer solution at a constant potential of 0.9 V after adding IFN-γ at different concentrations. (d) The calibration curve of the GC-ph-GO-aptamer(Ru) sensing interface obtained by the chronoamperometry in (c) and another two independent measurements. (e) I-t curves of aspirin at different concentrations of IFN-γ. (f) The standard linear calibration curve of cytokine according to (e) and another two independent measurements.

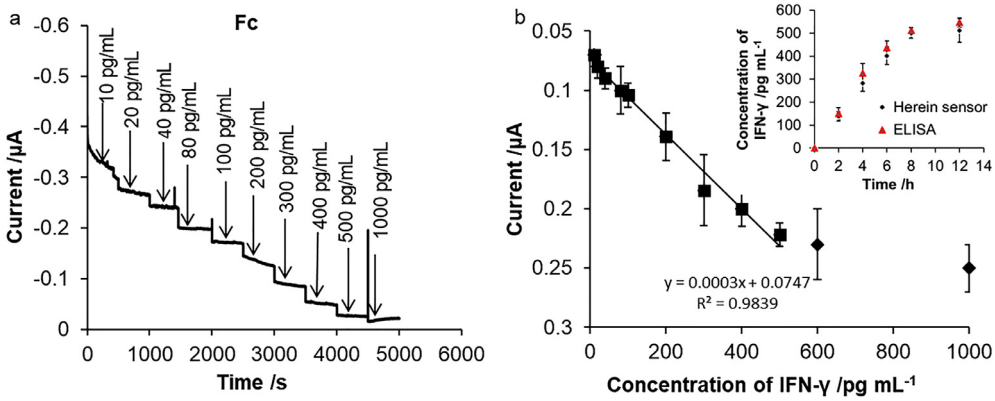

Fig. 6. (a) Chronoamperometry recording of GC-ph-STR-aptamer(aspirin) sensing cell culture media of PBMCs at a constant potential of 0.2 V after LPS treatment. (b) Calibration curve of the GC-ph-STR-aptamer(aspirin) sensing interface obtained by chronoamperometry in (a) and another two independent measurements. The inset in (b) is a comparison of the IFN-γ secretion profile between the presented sensor and the traditional ELISA after 10 ng mL^{-1} LPS stimulation.

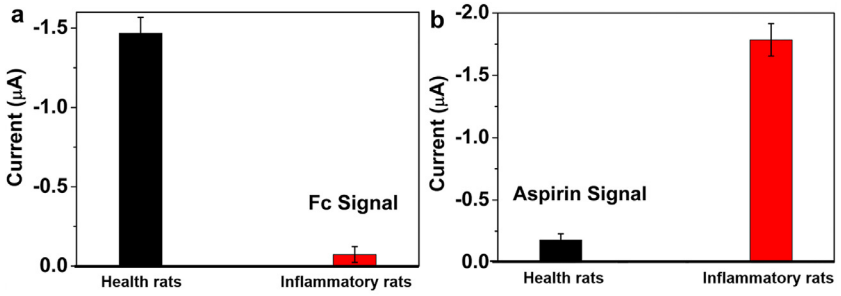

Fig. 7. Reduced Fc currents and increased aspirin currents measured in the blood of rats with inflammation using the GC-ph-STR-aptamer(aspirin) sensor. Currents generated at constant potentials of 0.2 V (a) and 0.9 V (b) were measured.

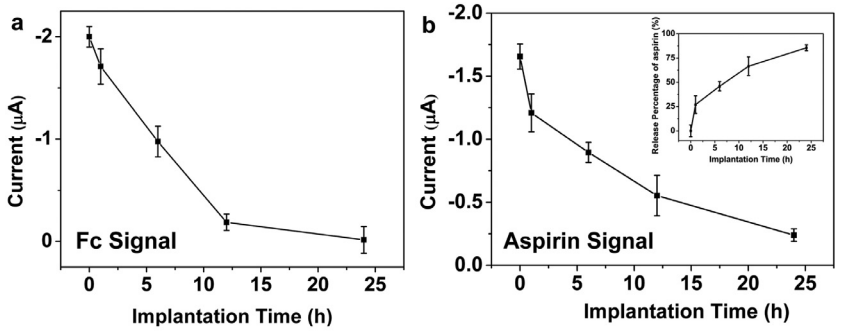

Fig. 8. Relationship between peak current and implantation time, which was obtained by the SWV measurement of the GC-ph-STR-aptamer(aspirin) device after implantation into the inflammatory rat model for different time points, in Tris–HCl buffer with the potential between 0 V and 0.5 V (a) and in Tris–HCl buffer containing 1000 pg/mL of IFN-γ with the potential between 0.7 V and 1.2 V (b). (a) Fc signal on the electrode and (b) the residual aspirin on the electrode. The inset shows the release profile of aspirin against the implantation time calculated from (b).

8 h LPS stimulation, a finding that was consistent to what we previously reported. [30] A comparison of IFN-γ detection using the proposed biosensor device and the traditional ELISA method is included in the inset of Fig. 6b. The sensor reported herein and ELISA displayed similar IFN-γ secretion patterns, suggesting that the performance of the sensor was comparable with that of ELISA for the detection of IFN-γ in a cell microenvironment.

3.6. Detection of IFN-γ and IFN-γ-triggered aspirin release in blood samples

The performance of the GC-ph-STR-aptamer(aspirin) for the detection of IFN-γ and simultaneous aspirin release was investigated in blood samples obtained from male rats intraperitoneally injected with LPS to induce endotoxemia (designated "inflammatory rat"). Blood samples were collected using heparinized capillary tubes at 0 h and 24 h after implantation. The GC-ph-STR-aptamer(aspirin)-modified *in vivo* devices were incubated in 1 mL of the blood collected from normal rats and the inflammatory rat model for 1 h. Then 1 mL of Tris–HCl buffer was added, and the chronoamperometry experiment at a constant potential of 0.2 V (Fc) and 0.9 V (aspirin) was performed utilizing these blood samples. As shown in Fig. 7 and Supplementary Figure S3, the monitored current of the GC-ph-STR-aptamer(aspirin) for the Fc peak in the blood of normal rats was much higher than that measured in the blood of the inflammatory rat model, while a completely contrasting phenomenon was observed in the current for the aspirin peak. This observation suggested that IFN-γ levels in the blood of the inflammatory rat model were much higher than those measured in the blood of normal rats. These results also demonstrated that only IFN-γ in the blood of the inflammatory rat model was able to release the aspirin from the GC-ph-STR-aptamer, thereby changing the configuration of aptamer to suppress the electrochemical signal of Fc. This demonstrated the potential of the GC-ph-STR-aptamer(aspirin) sensing device for the integrative detection of pro-inflammatory signals and subsequent therapy.

3.7. Detection of IFN-γ and IFN-γ-triggered aspirin release in living rats

To further investigate the *in vivo* performance of the GC-ph-STR-aptamer(aspirin) device for IFN-γ detection and aspirin release, the electrodes were initially implanted into the subcutaneous tissue of rats treated with LPS for 0–24 h. Then the withdrawn electrodes were measured by SWV in Tris-HCl buffer with the potential between −0 V and 0.5 V and in Tris-HCl buffer containing 1000 pg mL^{-1} of IFN-γ with the potential between 0.7 V and 1.2 V to check the remnant Fc and aspirin signal using procedures identical to those detailed above. As shown in Fig. 8 and Supplementary Figure S3, the SWV curves and current peak of the GC-ph-STR-aptamer(aspirin) devices against the implantation time in LPS-treated rats display dramatic peak current drops with time extension. The gradually decrease in the Fc and aspirin signals, respectively, demonstrated the specific detection of our sensor of inflammation (i.e., IFN-γ expression) and the inflammation-triggered aspirin release. Moreover, the difference in peak current between the untreated electrode (from the original aspirin) and the withdrawn electrodes (from the remnant aspirin) was used to calculate the percentage of aspirin release during the treatment. The consequence of the *in vivo* binding of IFN-γ on the GC-ph-STR-aptamer(aspirin) electrode was the immediate release of aspirin. The relationship between the release percentage of aspirin and the treatment time was also obtained (Fig. 8), revealing the prospect of the sensor for *in vivo* detection and subsequent aspirin delivery targeted to the treatment of inflammation. As shown in the inset of Fig. 8, the *in vivo* release efficiency of aspirin could reach up to 85.6% after 24 h. Considering that the body weight of rats used herein was approximately 180 g, each electrode would

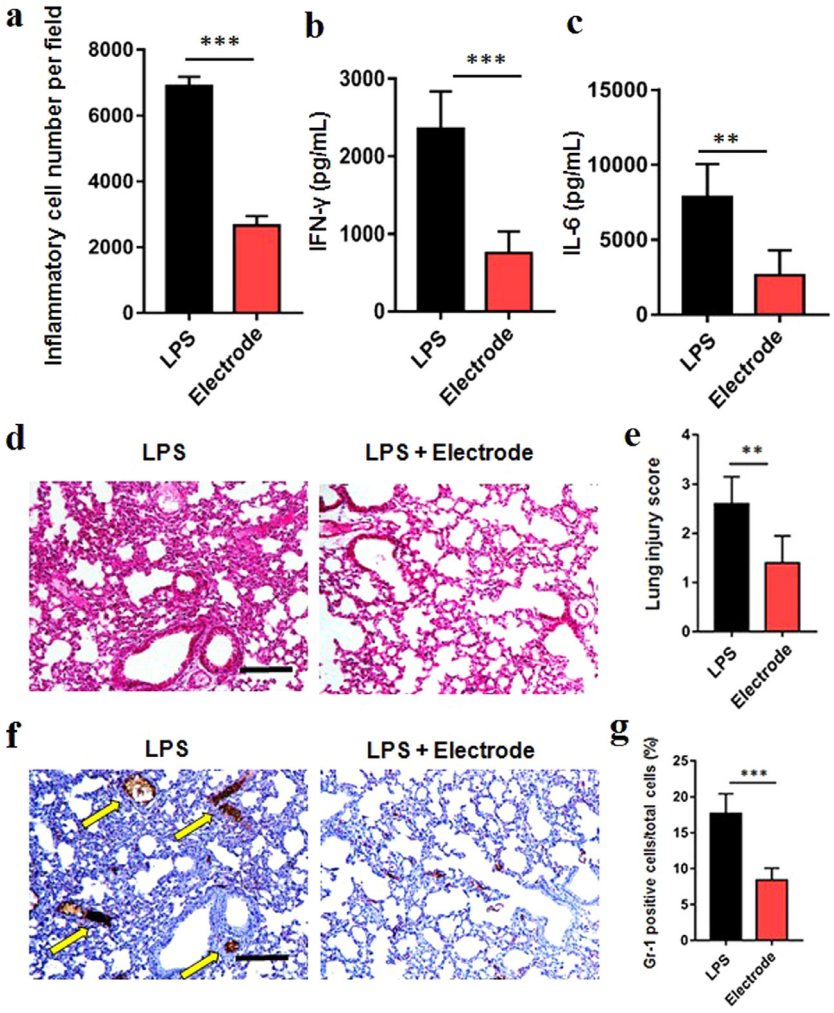

Fig. 9. (a) The quantification of inflammatory cells per field of lung tissue. (b-c) Expression level of inflammatory cytokines (IFN-γ and IL-6) in the interstitial fluid of the lung tissue by ELISA. (d) Histological analysis indicated that LPS injection caused capillary expansion and congestion, as well as neutrophil infiltration into the lung tissue, while the lung injury was well controlled by applying the electrode. The scale bar is 100 µm. (e) Lung injury score increased significantly after LPS administration and significantly reduced after electrode treatment (**, $p < 0.01$ compared with the LPS group). (f) Immunohistochemically identified neutrophils in the lung after LPS administration and electrode treatment. Yellow arrows represent the positive area. The scale bar is 100 µm. (g) Score of Ly-6 G protein expression levels increased in the lung sections of two groups (**, $p < 0.01$ compared with the LPS group). (For interpretation of the references to colour in this figure legend, the reader is referred to the web version of this article.)

release an aspirin level of 2.7 mg/kg in rat blood after 24 h of implantation. This aspirin concentration was lower than the ideal amount (10 mg/kg/day) used for traditionally anti-inflammatory treatment in a murine model [42].

3.8. In vivo *inflammation control using the adaptive GC-ph-STR-aptamer (aspirin) devices*

LPS is the major element of the outer membrane in gram-negative bacteria. LPS-induced endotoxemia can lead to serious acute lung injury (ALI), which is characterized by an increase in capillary permeability and neutrophil migration into the lungs [43]. Moreover, exposure to LPS can induce the secretion of additional proinflammatory cytokines, resulting in the activation of polymorphonuclear neutrophils (PMNs) and further inflammatory responses in the lung [44]. To demonstrate the performance of adaptive GC-ph-STR-aptamer(aspirin) *in vivo* devices, we collected lungs from the inflammatory rat model with and without electrode implantation for 24 h, and then the quantitative analysis of these lung samples was performed to provide evidence for the *in vivo* therapeutic efficacy of our electrode. As shown in Fig. 9a, the number of inflammatory cells was significantly reduced after electrode administration under LPS treatment condition. In addition, the ELISA results show that the expression of inflammatory cytokines (IFN-γ and IL-6) in the interstitial fluid obviously deregulated, indicating the effective inhibition of the inflammation (Fig. 9b and c). These lung samples were also stained with hematoxylin and eosin (H&E) for histological analysis and neutrophil marker (Ly-6G) for polymorphonuclear (PMN) leukocyte infiltration *by* immunohistochemistry detection, indicating that PMN cells infiltrated more into the lungs of the untreated group 24 h after LPS injection than those of the electrode-treated group (Fig. 9d and f). Moreover, Fig. 9e and g show that the degree of lung injury was significantly improved while the number of neutrophil expression was dramatically reduced after treatment with our electrode, providing further evidence of the therapeutic efficacy of our electrode.

To further evaluate the therapy, the blood specimens of the electrode-treated and untreated inflammatory rat model were collected for the measurement of the inflammatory cytokines IFN-γ and IL-6. As shown in Fig. 10, the levels of inflammatory cytokines (IL-6 and IFN-γ) in the electrode-treated rats have no obvious change within 24 h after LPS injection, which is in accordance with

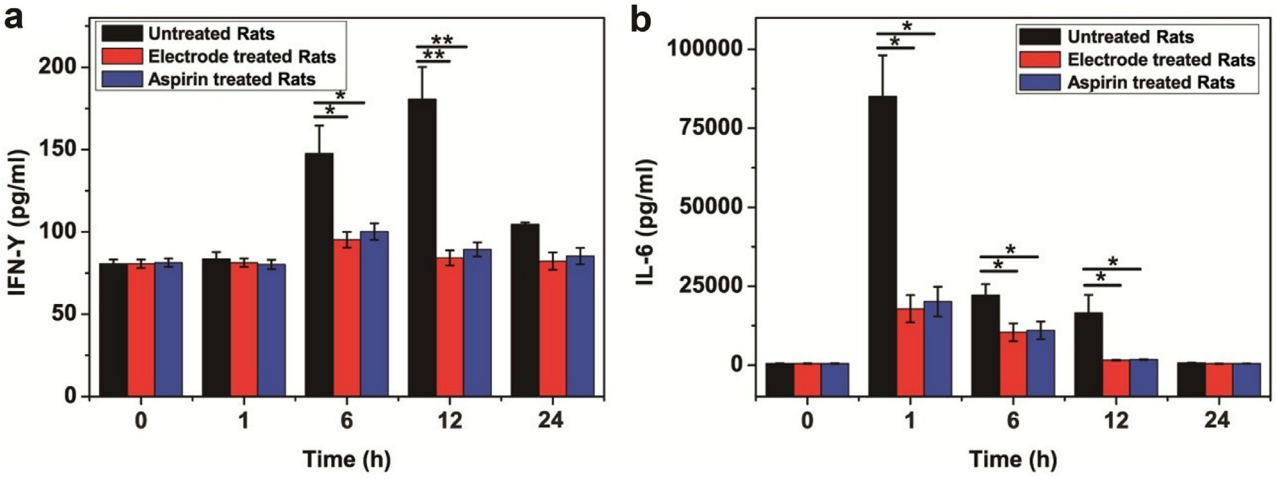

Fig. 10. The inflammation induced by LPS (control, untreated group) was inhibited by the GC-ph-STR-aptamer(aspirin) sensor (electrode-treated group) or pure aspirin (aspirin-treated group). The concentration of IFN-γ (a) and IL-6 (b) was measured in the serum of the inflammatory rat model with and without treatments.

the pure aspirin-treated rats. However, the concentration of both inflammatory cytokines in rats without treatment dramatically increased only in several hours. This indicates that the inflammation could be effectively and consistently suppressed by application of our electrodes. These results revealed that this adaptive GC-ph-STR-aptamer(aspirin) *in vivo* device could achieve the on-demand release of aspirin to effectively inhibit inflammation.

4. Conclusions

Cytokines, the signaling molecules in the immune system, play a key role in mediating and controlling immune and inflammatory responses. [45] Complex interactions exist among cytokines, inflammation, and the adaptive and innate responses to maintain normal homeostasis. It is essential to develop accurate and sensitive methods for the measurement of cytokines in real time to dynamically monitor inflammation, and such measurements can be an important basis for the proper treatment of developing and ongoing disease. [22,30,46] Recently, there has been increasing evidence that an abnormal inflammatory response is closely associated with various disease conditions. [1] Thus, interest has been shown toward therapeutically targeting the inflammatory response. Lack of precise, directed application of therapeutics and reduced effectiveness with chronic use are current limitations for the treatment of inflammation. To overcome these issues, precision or personalized medicine has demonstrated the capability of diagnosis and triggered treatment by delivering “the right drug, at the right dose, and at the right time” [6].

On-demand, local delivery of anti-inflammatory drugs to target tissues provides a means for effective drug dosing while reducing the adverse effects of systemic drug delivery. The study reported here has demonstrated a proof-of-concept theranostic approach for inflammation based on analyte-kissing-induced signaling whereby a drug (in this report, aspirin) can be released upon the detection of a target level of a proinflammatory cytokine (i.e., interferon-γ (IFN-γ)) in real time. The structure-switching aptamer-based biosensor described here is capable of quantitatively and dynamically detecting IFN-γ both *in vitro* and *in vivo* with a sensitivity of 10 pg mL^{-1}. Moreover, the released aspirin triggered by the inflammatory cytokine IFN-γ is able to inhibit inflammation in a rat model, and the release of aspirin can be quantitatively controlled. This study is a an advancement of our previous study that reported a sensitive sensing device for monitoring inflammation in mice. [30] In our previous report, the positively charged redox probes (ruthenium hexamine), acting as the signaling molecules, were loaded into the structure-switching aptamers. The presence of IFN-γ triggers the release of redox probes, resulting in an electrochemical signal that measures the concentration of IFN-γ. Although the sensitivity of this sensor is high, this *in vivo* sensing device has three limitations: 1) it cannot act as a real-time sensor, 2) the release of redox probes into the mice might cause a potential safety problem, and 3) it does not have the therapeutic function of the device reported in this study.

Specifically, here we prepared the adaptive device based on the aspirin intercalating hairpin aptamer that can realize the spatially localized monitoring of IFN-γ in real time along with the simultaneous delivery of aspirin. Furthermore, the performance of this adaptive device has been investigated *in vitro*, in cell culture medium, in blood samples, and in the serum of LPS-treated rats. To the best of our knowledge, this is the first study to provide a technology for the *in vivo* real-time monitoring of proinflammatory cytokines and the subsequent therapeutic delivery of anti-inflammatory molecules. Thus, this report provides a new and promising strategy for *the* precision theranostic of inflammation. By varying the aptamer probes targeted to different analytes (such as cancer biomarkers) and also the availability of small therapeutic drugs (such as doxorubicin), this universal theranostic platform has significant potential for personalized medicine and the effective treatment of numerous health conditions.

Declaration of Competing Interest

None.

Acknowledgments

This work was financially supported by the National Natural Science Foundation of China (Grant no. 21575045), the ARC Future Fellowship (FT160100039), and the ARC Centre of Excellence for Nanoscale BioPhotonics (CE140100003). The content of this publication does not necessarily reflect the views or policies of the U.S. Department of Health and Human Services nor does mention of trade names, commercial products, or organizations imply endorsement by the U.S. Government.

Supplementary material

Supplementary material associated with this article can be found, in the online version, at doi:10.1016/j.actbio.2019.10.021.

References

[1] P. Hunter, The inflammation theory of disease: the growing realization that chronic inflammation is crucial in many diseases opens new avenues for treatment, EMBO Rep. 13 (11) (2012) 968–970.
[2] S.I. Grivennikov, F.R. Greten, M. Karin, Immunity, inflammation, and cancer, Cell 140 (6) (2010) 883–899.
[3] G. Pawelec, D. Goldeck, E. Derhovanessian, Inflammation, ageing and chronic disease, Curr. Opin. Immunol. 29 (2014) 23–28.
[4] I. Tabas, C.K. Glass, Anti-inflammatory therapy in chronic disease: challenges and opportunities, Science 339 (6116) (2013) 166–172.
[5] A. Muraro, W.J. Fokkens, S. Pietikainen, D. Borrelli, I. Agache, J. Bousquet, V. Costigliola, G. Joos, V.J. Lund, L.K. Poulsen, European symposium on precision medicine in allergy and airways diseases: report of the European union parliament symposium (October 14, 2015), Rhinology 71 (5) (2015) 583–587.
[6] M.A. Hamburg, F.S. Collins, The path to personalized medicine, N. Engl. J. Med. 363 (4) (2010) 301.
[7] M. Twilt, Precision medicine: the new era in medicine, EBioMedicine 4 (2016) 24–25.
[8] P.W. Hellings, W.J. Fokkens, C. Bachert, C.A. Akdis, T. Bieber, I. Agache, M. Bernal-Sprekelsen, G.W. Canonica, P. Gevaert, G. Joos, Positioning the principles of precision medicine in care pathways for allergic rhinitis and chronic rhinosinusitis-an EUFOREA-ARIA-EPOS-AIRWAYS ICP statement, Allergy (2017).
[9] S. Borkowski, L.M. Dinkelborg, Aptamers for In Vivo Imaging, Wiley-VCH Verlag GmbH & Co. KGaA, 2006.
[10] S. Sarah, M. Joanna, O.C. Michael, W. Tao, D. Xiang, A.S. Hadi, Q. Liang, W. Ming, S.F. Zhou, Y. Zhu, Aptamers as theranostic agents: modifications, serum stability and functionalisation, Sensors 13 (10) (2013) 13624–13637.
[11] C. Song, Z.-G. Wang, B. Ding, in: Design, Fabrication, and Applications of DNA Nanomachines, DNA Nanotechnology, Springer, 2013, pp. 225–261.
[12] K.W. Plaxco, H.T. Soh, Switch-based biosensors: a new approach towards real–time, *in vivo* molecular detection, Trends Biotechnol. 29 (1) (2011) 1.
[13] N. Arroyo-Currás, J. Somerson, P.A. Vieira, K.L. Ploense, T.E. Kippin, K.W. Plaxco, Real-time measurement of small molecules directly in awake, ambulatory animals, Proc. Natl. Acad. Sci. 114 (4) (2017) 645–650.
[14] B.S. Ferguson, D.A. Hoggarth, D. Maliniak, K. Ploense, R.J. White, N. Woodward, K. Hsieh, A.J. Bonham, M. Eisenstein, T.E. Kippin, Real-time, aptamer-based tracking of circulating therapeutic agents in living animals, Sci. Trans. Med. 5 (213) (2013) 213ra165–213ra165.
[15] S. Vellampatti, R. Heo, M.S. Babu, J.H. Park, S.H. Park, Aptamer-conjugated DNA nano-ring as the carrier of drug molecules, Nanotechnology 29 (9) (2017).
[16] J.D.V. Willem, S. Schnichels, J. Hurst, L. Strudel, A. Gruszka, M. Kwak, K.U. Bartzschmidt, M.S. Spitzer, A. Herrmann, DNA nanoparticles for ophthalmic drug delivery, Biomaterials 157 (2018) 98–106.
[17] W. Tan, H. Wang, Y. Chen, X. Zhang, H. Zhu, C. Yang, R. Yang, C. Liu, Molecular aptamers for drug delivery, Trends Biotechnol. 29 (12) (2011) 634–640.
[18] S. Ranallo, C. Prévost-Tremblay, A. Idili, A. Vallée-Bélisle, F. Ricci, Antibody-powered nucleic acid release using a DNA-based nanomachine, Nat. Commun. 8 (2017) 15150.
[19] C. Angell, M. Kai, S. Xie, X. Dong, Y. Chen, Bioderived dna nanomachines for potential uses in biosensing, diagnostics, and therapeutic applications, Adv. Healthc. Mater. (2018).
[20] The Molecular Biology of Cytokines. J. Wiley, 1998.
[21] M.D. Turner, B. Nedjai, T. Hurst, D.J. Pennington, Cytokines and chemokines: at the crossroads of cell signalling and inflammatory disease, Biochim. Biophys. Acta, (BBA)-Molecular Cell Research 1843 (11) (2014) 2563–2582.
[22] G. Liu, Q. Meng, M.R. Hutchinson, G. Yang, E.M. Goldys, Recent advances in cytokine detection by immunosensing, Biosens. Bioelectron 79 (2) (2016) 810.
[23] H. Wei, S. Ni, C. Cao, G. Yang, G. Liu, Graphene oxide signal reporter based multifunctional immunosensing platform for amperometric profiling of multiple cytokines in serum, ACS Sens. 3 (8) (2018) 1553–1561.
[24] M. Qi, J. Huang, H. Wei, C. Cao, S. Feng, Q. Guo, E.M. Goldys, R. Li, G. Liu, Graphene oxide thin film with dual function integrated into a nanosandwich device for in vivo monitoring of interleukin-6, ACS Appl. Mater. Interfaces 9 (48) (2017) 41659–41668.
[25] M. Qi, Y. Zhang, C. Cao, M. Zhang, S. Liu, G. Liu, Decoration of reduced graphene oxide nanosheets with aryldiazonium salts and gold nanoparticles toward a label-free amperometric immunosensor for detecting cytokine tumor necrosis factor-α in live cells, Anal. Chem. 88 (19) (2016) 9614–9621.
[26] G. Liu, K. Zhang, K. Ma, A. Care, M.R. Hutchinson, E.M. Goldys, Graphene quantum dot based “switch-on” nanosensors for intracellular cytokine monitoring, Nanoscale 9 (15) (2017) 4934–4943.
[27] K. Ma, F. Zhang, N. Sayyadi, W. Chen, A.G. Anwer, A. Care, B. Xu, W. Tian, E.M. Goldys, G. Liu, “Turn-on” fluorescent aptasensor based on AIEgen labeling for the localization of IFN-γ in live cells, ACS Sens. 3 (2) (2018) 320–326.
[28] C. Cao, R. Jin, H. Wei, W.-C. Yang, E.M. Goldys, M.R. Hutchinson, S. Liu, X. Chen, G.-F. Yang, G. Liu, Graphene oxide based recyclable *in vivo* device for amperometric monitoring of interferon-γ in inflammatory mice, ACS Appl. Mater. Interfaces 10 (39) (2018) 33078–33087.
[29] A.R. Amin, M.G. Attur, M. Pillinger, S.B. Abramson, The pleiotropic functions of aspirin: mechanisms of action, Cell. Mol. Life Sci. 56 (3–4) (1999) 305–312.
[30] J. Li, D. Li, X. Liu, S. Tang, F. Wei, Human umbilical cord mesenchymal stem cells reduce systemic inflammation and attenuate LPS-induced acute lung injury in rats, J. Inflamm. 9 (33) (2012) 1–11.
[31] T. Yoshida, K. Nagai, T. Inomata, Y. Ito, T. Betsuyaku, M. Nishimura, Relationship between neutrophil influx and oxidative stress in alveolar space in lipopolysaccharide-induced lung injury, Respir. Physiol. Neurobiol. 191 (2014) 75–83.
[32] C.V. Kulkarni, V.K. Vishwapathi, A. Quarshie, Z. Moinuddin, J. Page, P. Kendrekar, S.S. Mashele, Self-Assembled lipid cubic phase and cubosomes for the delivery of aspirin as a model drug, Langmuir (2017) 9907–9915.
[33] J.F. Neault, M. Naoui, M. Manfait, H.A. Tajmir-Riahi, Aspirin-DNA interaction studied by FTIR and laser Raman difference spectroscopy, FEBS Lett. 382 (1–2) (1996) 26–30.
[34] R. Elghanian, J.J. Storhoff, R.C. Mucic, R.L. Letsinger, C.A. Mirkin, Selective colorimetric detection of polynucleotides based on the distance-dependent optical properties of gold nanoparticles, Science 277 (5329) (1997) 1078–1081.
[35] G. Liu, Q. Meng, Y. Zhang, C. Cao, E.M. Goldys, Nanocomposites of gold nanoparticles and graphene oxide towards an stable label-free electrochemical immunosensor for detection of cardiac marker troponin-I, Anal. Chim. Acta 909 (2016) 1–8.
[36] K. Gajos, P. Petrou, A. Budkowski, K. Awsiuk, A. Bernasik, K. Misiakos, J. Rysz, I. Raptis, S. Kakabakos, Imaging and spectroscopic comparison of multi-step methods to form DNA arrays based on the biotin-streptavidin system, Analyst 140 (4) (2015) 1127–1139.
[37] S. Bizid, S. Blili, R. Mlika, A.S. Haj, H. Korriyoussoufi, Direct electrochemical DNA sensor based on a new redox oligomer modified with ferrocene and carboxylic acid: application to the detection of mycobacterium tuberculosis mutant strain, Anal. Chim. Acta 994 (2017) 10.
[38] A. Erdem, P. Papakonstantinou, H. Murphy, M. Mcmullan, H. Karadeniz, S. Sharma, Streptavidin modified carbon nanotube based graphite electrode for label-free sequence specific DNA detection, Electroanalysis 22 (6) (2010) 611–617.
[39] K.L. Hamner, C.M. Alexander, K. Coopersmith, D. Reishofer, C. Provenza, M.M. Maye, Using temperature-sensitive smart polymers to regulate DNA-mediated nanoassembly and encoded nanocarrier drug release, ACS Nano 7 (8) (2013) 7011–7020.
[40] J.A. Ramos-Vara, M.A. Miller, When tissue antigens and antibodies get along: revisiting the technical aspects of immunohistochemistry–the red, brown, and blue technique, Vet. Pathol. 51 (1) (2014) 42–87.
[41] H. Sun, M.S. Chow, A method of determining the *in vivo* drug release rate constant of sustained-release preparation, Drug Metab. Dispos. Biol. Fate Chem. 23 (4) (1995) 449–454.
[42] D.W. Gilroy, A. Tomlinson, D.A. Willoughby, Differential effects of inhibitors of cyclooxygenase (cyclooxygenase 1 and cyclooxygenase 2) in acute inflammation, Eur. J. Pharmacol. 355 (1998) 211–217.
[43] G. Matute-Bello, C.W. Frevert, T.R. Martin, Animal models of acute lung injury, Am. J. Physiol. Lung Cell Mol. Physiol. 295 (3) (2008) L379–L399.
[44] H. Lv, Q. Liu, Z. Wen, H. Feng, X. Deng, X. Ci, Xanthohumol ameliorates lipopolysaccharide (LPS)-induced acute lung injury via induction of AMPK/GSK3beta-Nrf2 signal axis, Redox Biol. 12 (2017) 311–324.
[45] C.A. Dinarello, Historical review of cytokines, Eur. J. Immunol. 37 (Suppl 1) (2007) S34.
[46] C. Cao, F. Zhang, E.M. Goldys, F. Gao, G. Liu, Advances in structure-switching aptasensing towards real time detection of cytokines, TrAC Trends Anal. Chem. 102 (2018) 379–396.